INTERNATIONAL JOURNAL FOR NUMERICAL METHODS IN FLUIDS
Int. J. Numer. Meth. Fluids 2000; **32**: 585–604

Simulation of unsteady turbulent flows around moving aerofoils using the pseudo-time method

K. J. Badcock*, F. Cantariti, I. Hawkins, M. Woodgate, L. Dubuc and B. E. Richards

Department of Aerospace Engineering, University of Glasgow, Glasgow, G12 8QQ, U.K.

SUMMARY

The pseudo-time formulation of Jameson has facilitated the use of numerical methods for unsteady flows, these methods have proved successful for steady flows. The formulation uses iterations through pseudo-time to arrive at the next real time approximation. This iteration can be used in a straightforward manner to remove sequencing errors introduced when solving mean flow equations together with another set of differential equations (e.g. two-equation turbulence models or structural equations). The current paper discusses the accuracy and efficiency advantages of removing the sequencing error and the effect that building extra equations into the pseudo-time iteration has on its convergence characteristics. Test cases used are for the turbulent flow around pitching and ramping aerofoils. The performance of an implicit method for solving the pseudo-steady state problem is also assessed. Copyright © 2000 John Wiley & Sons, Ltd.

KEY WORDS: pseudo-time method; turbulent flow; unsteady flow

1. INTRODUCTION

A range of methods has been developed for solving the steady state Reynolds-averaged Navier–Stokes (RANS) equations. These include multigrid methods, local time stepping and approximate iteration schemes, all of which are concerned with either reducing the number of time steps to convergence or reducing the cost of these steps. For unsteady flows, the number of time steps required is fixed by the need to satisfactorily follow the evolution of the flow. There is no direct generalization of the successful methods from steady state problems since these destroy the time accuracy, which is the essential requirement of the calculation.

A fundamental design criterion for a numerical method to solve the unsteady RANS equations can be stated as

* Correspondence to: Department of Aerospace Engineering, University of Glasgow, James Watt Building, Glasgow G12 8QQ, U.K.

CCC 0271–2091/2000/050585–20$17.50

Received August 1998
Revised January 1999

'The time step is chosen to ensure time accuracy with no efficiency or stability restriction.'

The idea put forward by Jameson [1] established a framework, referred to here as pseudo-time, in which this can be achieved. The calculation of the flow solution at each time step involves the solution of a reformulated steady state problem, which can be computed using the acceleration techniques that have proved successful for steady flows. Applications of this approach for inviscid compressible flows include using explicit time stepping [2], multigrid and unstructured meshes [3] and an implicit solver [4]. The pseudo-time method has been applied for the simulation of turbulent flow around oscillating wings, where the pseudo-time iterations are frequently referred to as *sub-iterations*. These sub-iterations usually consist of factored implicit steps such as alternating direct implicit (ADI) [7] or LU-decomposition [8,9]. The calculation times quoted for these applications are often very lengthy, indicating the potential benefits of making the simulation more efficient.

When two-equation turbulence closure is used, the solution as one system [10] (i.e. fully coupled) of the mean flow and turbulence equations has disadvantages. It is often desirable to use different solution methods for the mean and turbulent flow equations. For example, an implicit method can be used to overcome the stiffness caused by the source term in the turbulence equations while an explicit method is used for the mean flow equations [11]. The alternative is to solve the equations in a sequenced fashion, with the mean flow values frozen for the solution of the turbulence equations and then the turbulent values frozen for the solution of the mean flow. This method, referred to herein as sequenced in real time, is the most commonly used coupling approach. It has the practical advantage of allowing codes for the mean flow and turbulence equations to be used in a modular fashion with minimal interaction, simplifying implementation and testing. An example application is the study of dynamic stall using the $k-\epsilon$ turbulence model [9]. If the sequencing is done in real time for unsteady calculations then the turbulent and mean flow values are always out of phase by one time step, introducing an additional source of error into the calculation. However, if the solution is sequenced in *pseudo-time* rather than real time then the advantages of the decoupled solution are retained and, at convergence, there is no sequencing error.

This paper investigates the use of the pseudo-time method to remove sequencing errors for the solution of turbulent flows. The advantages of this are examined for two turbulent flows over the pitching and ramping NACA0012 aerofoils. The paper continues with a description of the numerical formulation, followed by a discussion of the test cases, with comparison being made between the present results and experimental data. This comparison highlights the sensitivity of the computed moment history to the shock location, and hence the flow modelling, used. Issues surrounding the convergence to the pseudo-steady state are highlighted in Section 4 and a comparison of the performance of the two coupling methods is then given, followed by conclusions.

2. NUMERICAL FORMULATION

A model for the mean flow quantities in a planar, turbulent, compressible and unsteady flow is given by the RANS equations

$$\frac{\partial \mathbf{w}}{\partial t}+\frac{\partial(\mathbf{f}^i-\mathbf{f}^v)}{\partial x}+\frac{\partial(\mathbf{g}^i-\mathbf{g}^v)}{\partial y}=0 \tag{1}$$

where $\mathbf{w}=(\rho, \rho u, \rho v, e)$.

The influence of turbulence on the mean flow can be described by using the Boussinesq approximation, which relates the Reynolds' stress tensor linearly to the strain rate tensor. The constant of proportionality is called the eddy viscosity μ_t. The calculation of the eddy viscosity requires additional relations, which include mean flow values. A popular family of methods consists of two differential equations that balance the convection, diffusion, production and dissipation of quantities associated with the turbulence. For example, the $k-\omega$ model [13] is given by

$$\frac{\partial \mathbf{q}}{\partial t}+\frac{\partial(\mathbf{f}_T^i-\mathbf{f}_T^v)}{\partial x}+\frac{\partial(\mathbf{g}_T^i-\mathbf{g}_T^v)}{\partial y}=\mathbf{S} \tag{2}$$

where $\mathbf{q}=(\rho k, \rho\omega)$. The source term on the right hand side of the equations describes production and dissipation of k and ω. All of the vectors in Equation (2) involve mean flow values. The turbulence is characterized in these equations by k and ω with the eddy viscosity given by $\mu_t=\rho k/\omega$.

The semi-discrete form of Equations (1) and (2) can be written as

$$\frac{\mathrm{d}\mathbf{w}_{i,j}}{\mathrm{d}t}=\mathbf{R}_{i,j}$$

and

$$\frac{\mathrm{d}\mathbf{q}_{i,j}}{\mathrm{d}t}=\mathbf{Q}_{i,j}$$

where $\mathbf{R}$ and $\mathbf{Q}$ represent the discretization of the convective and diffusive terms. In general, multiblock grids are used in the current work although single block grid notation is used to avoid unnecessary complexity in the description of the method. The convective fluxes are discretized by Osher's method together with MUSCL extrapolation and Von Albada limiter, and the diffusive terms by using contour integrations based on the divergence theorem [12]. The source terms in the $k-\omega$ model are evaluated at cell centres. The cell residuals $\mathbf{R}$ and $\mathbf{Q}$ depend on the values of $\mathbf{w}$ and $\mathbf{q}$ in 13 neighbouring cells. Denoting the vector whose components consist of the mean and turbulent flow quantities in these 13 cells by $\tilde{\mathbf{w}}_{i,j}$ and $\tilde{\mathbf{q}}_{i,j}$, the spatial discretization can be written as $\mathbf{R}_{i,j}=\mathbf{R}_{i,j}(\tilde{\mathbf{w}}_{i,j}, \tilde{\mathbf{q}}_{i,j})$ and $\mathbf{Q}_{i,j}=\mathbf{Q}_{i,j}(\tilde{\mathbf{w}}_{i,j}, \tilde{\mathbf{q}}_{i,j})$.

Following the pseudo-time formulation [1], the updated mean flow solution is calculated by solving the steady state problems

$$\mathbf{R}_{i,j}^*=\frac{3\mathbf{w}_{i,j}^{n+1}-4\mathbf{w}_{i,j}^n+\mathbf{w}_{i,j}^{n-1}}{2\Delta t}+\mathbf{R}_{i,j}(\tilde{\mathbf{w}}_{i,j}^{k_m}, \tilde{\mathbf{q}}_{i,j}^{k_t})=0 \tag{3}$$

$$\mathbf{Q}^*_{i,j} = \frac{3\mathbf{q}^{n+1}_{i,j} - 4\mathbf{q}^{n}_{i,j} + \mathbf{q}^{n-1}_{i,j}}{2\Delta t} + \mathbf{Q}_{i,j}(\tilde{\mathbf{w}}^{l_m}_{i,j}, \tilde{\mathbf{q}}^{l_t}_{i,j}) = 0 \tag{4}$$

Here k_m, k_t, l_m and l_t give the time level of the variables used in the spatial discretization. Note that for the problems in this paper the grid is moved rigidly, but if grid deformation was required then time varying areas would be required [4] in the expression for the real time derivative in Equations (3) and (4). If $k_m = k_t = l_m = l_t = n+1$, then the mean and turbulent quantities are advanced in real time in a fully coupled manner. However, if $k_m = l_m = l_t = n+1$ and $k_t = n$ then the equations are advanced in sequence in real time, i.e. the mean flow is updated using frozen turbulence values and then the turbulent values are updated using the latest mean flow solution. This has the advantage that the only modification, when compared with the laminar case, to the discretization of the mean flow equations is the addition of the eddy viscosity from the previous time step. The turbulence model only influences the mean flow solution through the eddy viscosity and so any two-equation models can be used without modifying the mean flow solver. Hence, the implementation is simplified by using a sequenced solution in real time. However, the uncoupling could adversely effect the stability and accuracy of the real time stepping, with the likely consequence of limiting the size of the real time step that can be used.

Equations (3) and (4) represent a coupled non-linear system of equations. These can be solved by introducing an iteration through *pseudo-time* τ to the steady state, as given by

$$\frac{\mathbf{w}^{n+1,m+1}_{i,j} - \mathbf{w}^{n+1,m}_{i,j}}{\Delta\tau} + \frac{3\mathbf{w}^{k_m}_{i,j} - 4\mathbf{w}^{n}_{i,j} + \mathbf{w}^{n-1}_{i,j}}{2\Delta t} + \mathbf{R}_{i,j}(\tilde{\mathbf{w}}^{k_m}_{i,j}, \tilde{\mathbf{q}}^{k_t}_{i,j}) = 0 \tag{5}$$

$$\frac{\mathbf{q}^{n+1,m+1}_{i,j} - \mathbf{q}^{n+1,m}_{i,j}}{\Delta\tau} + \frac{3\mathbf{q}^{l_t}_{i,j} - 4\mathbf{q}^{n}_{i,j} + \mathbf{q}^{n-1}_{i,j}}{2\Delta t} + \mathbf{Q}_{i,j}(\tilde{\mathbf{w}}^{l_m}_{i,j}, \tilde{\mathbf{q}}^{l_t}_{i,j}) = 0 \tag{6}$$

where the mth pseudo-time iterate at the $n+1$th real time step are denoted by $\mathbf{w}^{n+1,m}$ and $\mathbf{q}^{n+1,m}$ respectively. The iteration scheme used only effects the efficiency of the method, and hence, we can sequence the solution in pseudo-time without compromising accuracy. For example, using explicit time stepping we can calculate $\mathbf{w}^{n+1,m+1}$ using $k_m = n+1, m$ and $k_t = n+1, m$ and $\mathbf{q}^{n+1,m+1}$ using $l_m = n+1, m+1$ and $l_t = n+1, m$. For implicit time stepping in pseudo-time we can use $k_m = l_m = l_t = n+1, m+1$ and $k_t = n+1, m$. In both of these cases the solution of the equations is decoupled by freezing values, but at convergence the real time stepping proceeds with no sequencing error. It is easy to recover a solution which is sequenced in real time from this formulation by setting $k_t = n$ throughout the calculation of the pseudo-steady state. This facilitates a comparison of the current pseudo-time sequencing with the more common real time sequencing.

3. METHOD FOR CALCULATING PSEUDO-STEADY STATE

In this paper we use an implicit method to solve the pseudo-steady state problem. Using the notation of the previous section one pseudo-time step of the mean and turbulent solutions can be written

$$\frac{\mathbf{w}_{i,j}^{n+1,m+1} - \mathbf{w}_{i,j}^{n+1,m}}{\Delta\tau} + \frac{3\mathbf{w}_{i,j}^{n+1,m+1} - 4\mathbf{w}_{i,j}^{n} + \mathbf{w}_{i,j}^{n-1}}{2\Delta t} + \mathbf{R}_{i,j}(\tilde{\mathbf{w}}_{i,j}^{n+1,m+1}, \tilde{\mathbf{q}}_{i,j}^{n+1,m}) = 0 \tag{7}$$

$$\frac{\mathbf{q}_{i,j}^{n+1,m+1} - \mathbf{q}_{i,j}^{n+1,m}}{\Delta\tau} + \frac{3\mathbf{q}_{i,j}^{n+1,m+1} - 4\mathbf{q}_{i,j}^{n} + \mathbf{q}_{i,j}^{n-1}}{2\Delta t} + \mathbf{Q}_{i,j}(\tilde{\mathbf{w}}_{i,j}^{n+1,m+1}, \tilde{\mathbf{q}}_{i,j}^{n+1,m+1}) = 0 \tag{8}$$

These equations represent a non-linear system for $\mathbf{w}_{i,j}^{n+1,m+1}$ and $\mathbf{q}_{i,j}^{n+1,m+1}$ and are simplified by linearizing $\mathbf{R}_{i,j}(\tilde{\mathbf{w}}_{i,j}^{n+1,m+1}, \tilde{\mathbf{q}}_{i,j}^{n+1,m})$ and $\mathbf{Q}_{i,j}(\tilde{\mathbf{w}}_{i,j}^{n+1,m+1}, \tilde{\mathbf{q}}_{i,j}^{n+1,m+1})$ in pseudo-time [4]. The resulting linear systems are solving by a preconditioned conjugate gradient type method. Block incomplete lower upper (BILU) factorization is used as a preconditioner. It has been found to be more efficient to use an approximate linearization that saves memory and the cost of the matrix–vector products by reducing the number of non-zero elements in the coefficient matrix of the linear system. Full details of the method are identical to those used for solving the unsteady Euler equations [4].

The basic accuracy of the code has been tested for a number of applications. In Reference [5] steady state inviscid and laminar flow results for a NACA0012 aerofoil were compared with previously published results. In Reference [4] comparisons with experiment were made for three pitching cases over a NACA0012 aerofoil and also the steady state solution for the Williams two-element aerofoil was compared with a previously published potential flow solution. Detailed evaluation of the code for supersonic slender body aerodynamics and base flows has been made in Reference [6].

4. TEST CASES

The influence of solution coupling is considered for two test cases involving transonic flow over the NACA0012 aerofoil. For both cases the aerofoil rotates about the point at a quarter chord.

For the first case, called case CT2, the incidence as a function of time is given by

$$\alpha(t) = \alpha_m + \alpha_0 \sin(\omega_p t)$$

where $\alpha_m = 3.16°$, $\alpha_0 = 4.59°$ and $\omega_p = 0.16$. The free stream Mach number is 0.6 and the Reynolds number is 4.8 million.

A shock wave forms as the aerofoil pitches up and then weakens and disappears during the downward part of the cycle, as is evident from the pressure contours shown in Figure 1. The flow is fully attached throughout the motion. Excellent prediction of the pressure distributions (shown in Figure 2) and normal force and moment histories are possible and have been achieved here. Grid refinement was carried out on a sequence of grids derived from a fine grid with 513 points in the streamwise, and 129 points in the normal directions respectively. Medium and coarse grids were extracted from the fine grid by successively removing every second point. The medium grid was found to give a spatially well converged solution, as indicated in Figure 3 for the moment history. The time step refinement shown in Figure 4 shows that temporally 20 steps per cycle gives good accuracy. The comparison with experiment

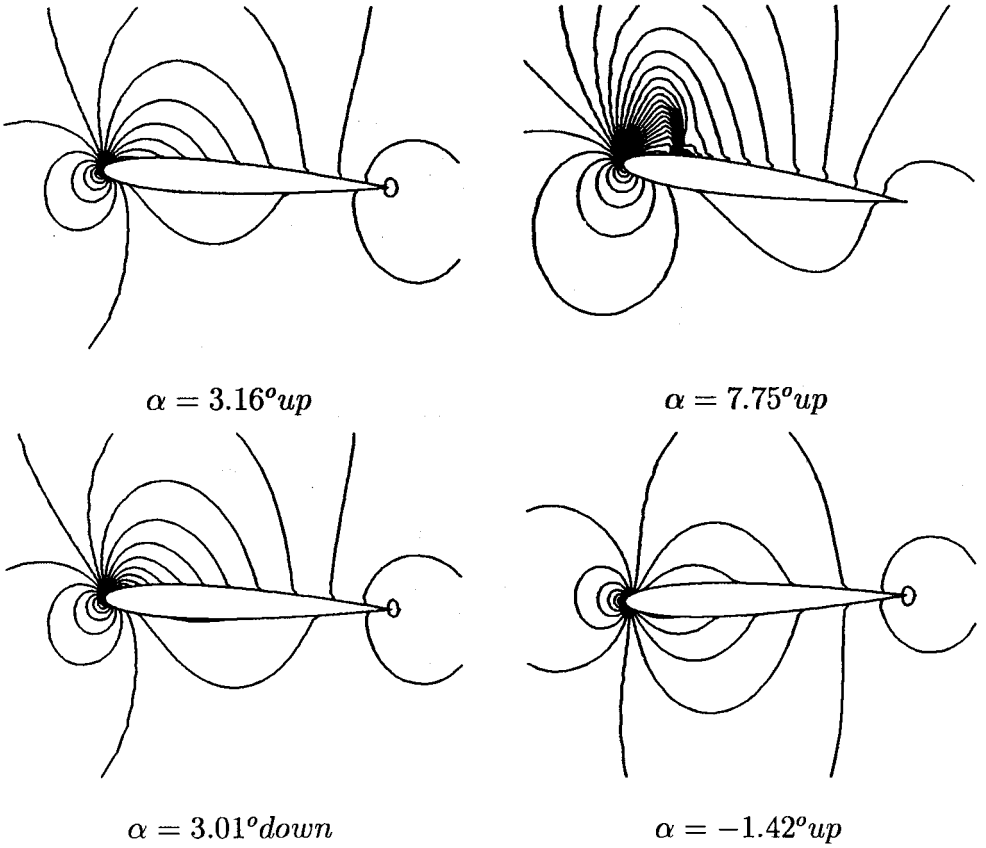

Figure 1. Pressure contours for case CT2.

[14] for the moment history is shown in Figure 5, on the fine grid using 20 steps per pitching cycle.

Several numerical studies of this case based on the Euler equations have suggested that the moment centre given in the experimental description is likely to be in error. The time history predicted by the Euler equations is also shown in Figure 6 and shows the discrepancy with the measured data when calculating the moment about $0.25c$ (where c is the aerofoil chord length), which is the stated location for the measurements. The difference becomes most marked at the larger angles of incidence when the shock wave is present. The moment location which consistently gives closer comparison between inviscid computations and measured values is $0.273c$ [2,4,15,16]. However, for the current turbulent results, it was found that using the quoted experimental moment centre at $0.25c$ gives close agreement with experimental measurements.

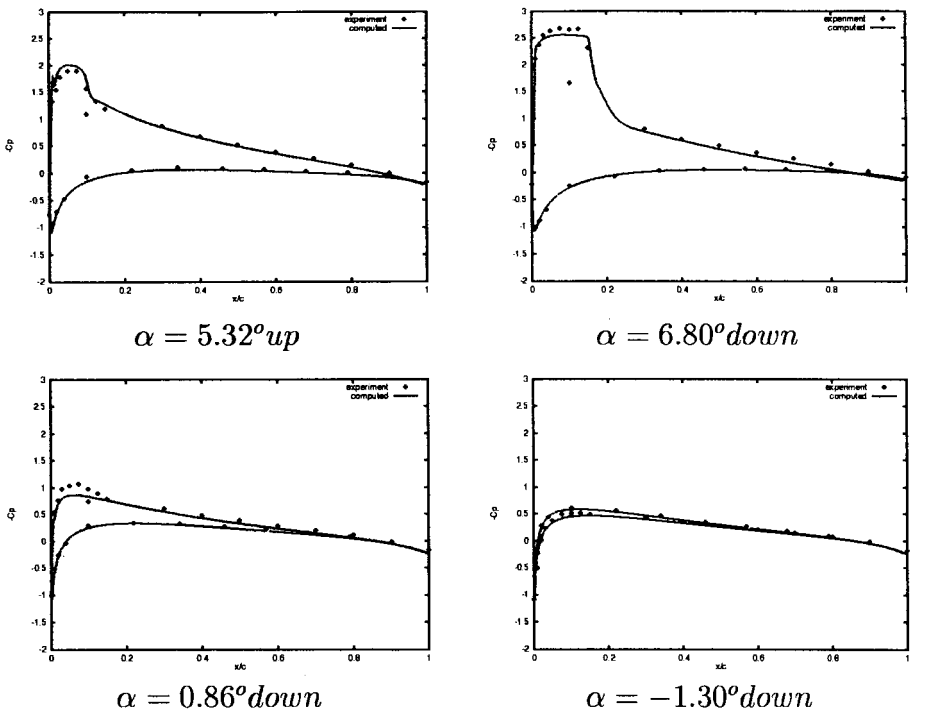

Figure 2. Instantaneous pressure distributions for case CT2.

The turbulent simulation predicts the shock wave further upstream than the inviscid one due to the displacement effect of the boundary layer (see Figure 7). Note that in both cases the shock is located upstream of the point $0.25c$. The effect of moving the moment centre and the shock closer together is to decrease the net nose-up moment. Since the inviscid calculation predicts the shock wave location to be slightly closer to the moment centre than in reality, the main effect of moving the moment centre to $0.273c$ for the inviscid results is to compensate for this error when calculating the moment. This has the effect of increasing the computed values of moment. The shock location from the present calculations is closer to the measured location, and hence, this correction is not necessary. A smaller moment is computed on the coarse grid since the jump across the shock is underpredicted. This effect can again be compensated for by moving the moment centre to $0.273c$. A previously published turbulent result [17] underpredicts the jump across the shock due to the coarseness of the grid, and hence, better agreement for this calculation is obtained between computed and measured moment values if the moment centre is moved aft to $0.273c$.

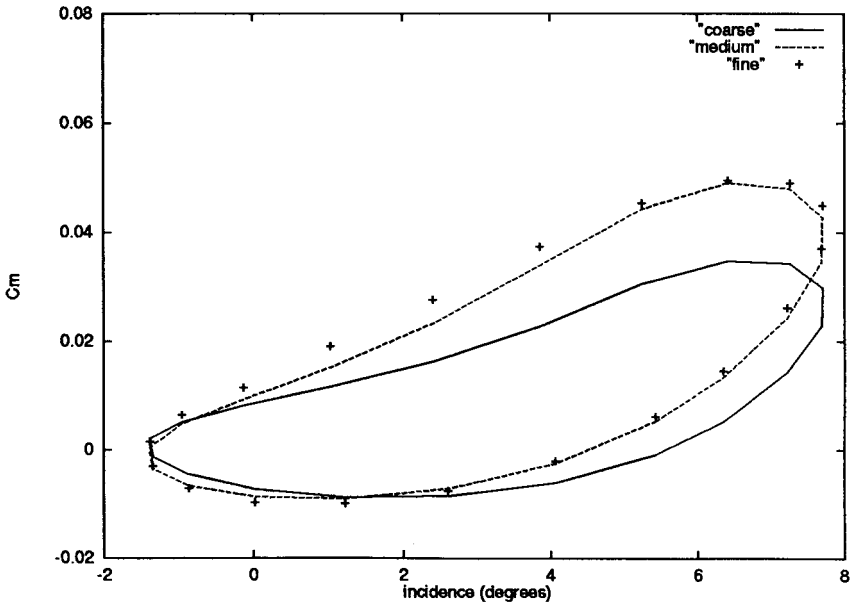

Figure 3. Grid convergence for integrated moment for case CT2.

The second test case involves a ramping motion and is referred to as CT8. The incidence is given by

$$\alpha(t) = \alpha_0 + k_r t$$

where $\alpha_0 = -0.01°$ and $k_r = 0.85°$ per time unit. The free stream Mach number is 0.59 and the Reynolds number is 4.5 million.

A shock wave strengthens near the leading edge (see Figure 8) as the aerofoil pitches up until the flow is induced to separate at around 8.3°. The separated region grows (see Figure 9 and the shock weakens and moves upstream until stall is reached just after 13°. The comparison of the computed pressure distributions with measured values indicates reasonable agreement until separation becomes the dominant flow feature, after which the linear turbulence modelling is inadequate (see Figure 10). The integrated forces and pressure distributions show good agreement with experiment up to separation, as shown in Figure 11. The location of stall is predicted earlier than observed in experiment. A grid refinement study, using the same methodology as for the pitching case, showed that the medium grid gives a well converged spatial solution, as shown in Figure 12. A time step leading to a motion of 0.170° gives a temporally well-converged solution, as shown in Figure 13.

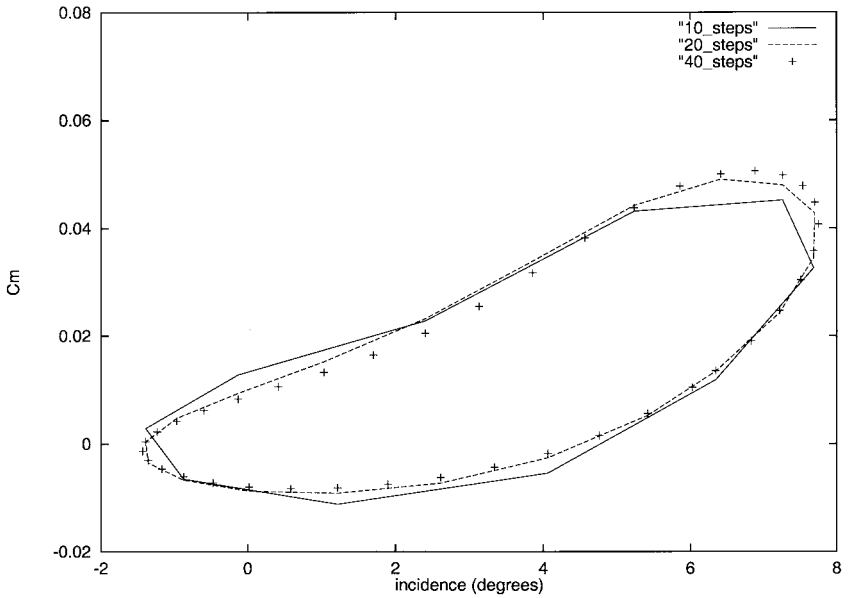

Figure 4. Convergence with number of real time steps per cycle for integrated moment for case CT2.

5. CONVERGENCE TO PSEUDO-STEADY STATE

The convergence to the updated flow solution is monitored by the ratio of the pseudo-time to the real time update

$$\frac{\left\|\mathbf{w}^{n+1,m+1}-\mathbf{w}^{n+1,m}\right\|_2}{\left\|\mathbf{w}^{n+1,m+1}-\mathbf{w}^{n}\right\|_2}$$

Values of 10^{-2} and 10^{-3} for the tolerance were used for both test problems and were found to give similar results. A value of 10^{-2} means that the latest pseudo-time update is less than 1 per cent of the resulting estimate to the real time update. The calculation with a tolerance of 10^{-3} takes roughly twice as long compared with using 10^{-2}, the value used for the results shown in this paper.

For all steady state time stepping methods it is advantageous to start the iterations as close to the converged solution as possible. For the implicit method it is necessary to have a good approximation to the converged solution before using large Courant–Friedrich–Lewy (CFL) numbers. For the pseudo-steady state problems the previous time step (i.e. $\mathbf{w}^{n+1,1}=\mathbf{w}^{n}$) provides an obvious choice for the starting solution. In an attempt to obtain a better initial solution, the use of extrapolation from previous real time levels was tested. The initial pseudo-time iterate was obtained by extrapolating the solutions from the two previous time levels (i.e. $\mathbf{w}^{n+1,1}=2\mathbf{w}^{n}-\mathbf{w}^{n-1}$). This approach was found to lead to negative pressure values in the vicinity of large shock motions and was rejected.

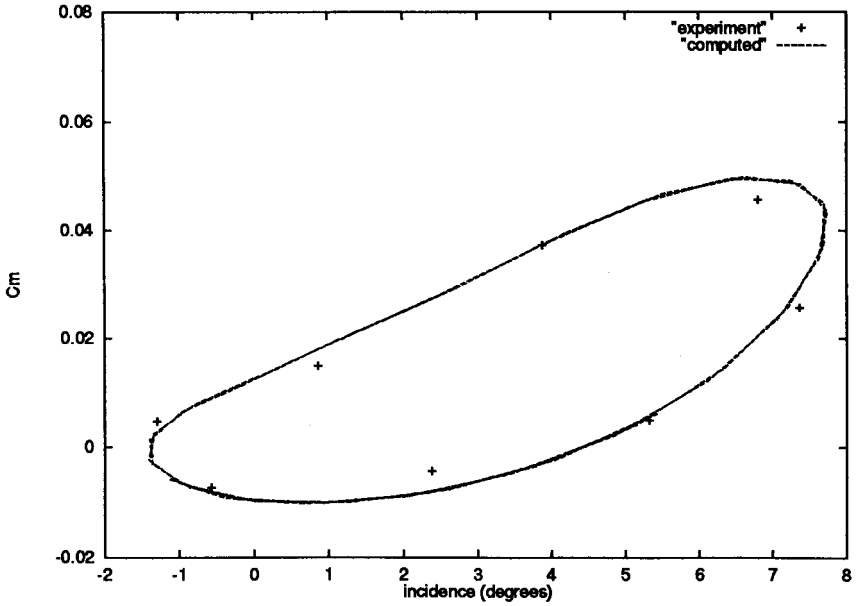

Figure 5. Comparison of integrated moment with experiment for case CT2.

The average cost of the pseudo-steady state calculation per real time step is less than 100 residual evaluations. This represents a cheap calculation when compared with normal flow steady state problems and indicates that using the solution from the previous time step as an initial condition for the next time step is satisfactory.

For the pseudo-steady state calculation method to be satisfactory the cost should decrease with an increasing time step, allowing the choice of time step from accuracy considerations alone. This cost is shown in Table I for various sizes of time step and it can be seen that the CPU time required does indeed decrease with increasing time step. The CPU time is expressed in terms of work units, where one work unit is the time required for one residual evaluation. The change in flow values between time steps would be expected to increase with the real time step, and hence, also the difficulty in obtaining the pseudo-steady state. It can be seen in Table I that as the time step is increased by a factor of 8 for the pitching case the average number of pseudo-time steps required to solve each steady state problem less than doubles. The cost of each pseudo-time iteration is also insensitive to the real time step used, and hence, the reduction in cost of the calculation as the time step is increased is due to the reduction in the number of real time steps being carried out. Similar conclusions are drawn for the ramping case.

It can be seen in Table II that the cost of the solution increases relatively as the grid is refined. This is due to the increasing number of pseudo-steps required to solve the pseudo-steady state problem. The cost of the linear solves does not increase with the grid refinement,

indicating the good quality of the BILU preconditioning. The influence of the complexity of the flow features on the difficulty in obtaining the pseudo-steady state is of interest when considering the extension to more complex applications. To examine this, the number of pseudo-steps is plotted as a function of incidence in Figures 14 and 15. For the pitching case, a clear increase in the number of pseudo-steps is observed as the shock wave develops while the aerofoil is pitching up. However, the cost of the steady state calculation only varies by a factor of two throughout the cycle.

For the ramping case, there is again an increase in the number of pseudo-steps required as the shock wave forms and strengthens. The cost then decreases as the separated region grows and the shock wave disappears. This indicates that shock waves are more important for determining the cost of solving the pseudo-steady state problem than regions of flow separation.

6. COMPARISON BETWEEN SEQUENCING IN REAL AND PSEUDO-TIME

The current formulation allows the use of solutions that are sequenced or coupled (i.e. sequenced in pseudo-time) in real time, and hence, the influence of the real time sequencing used in the majority of unsteady turbulent flow simulations can be assessed.

For the pitching case, no solution was obtained using a sequenced solution in real time for 10 and 20 steps per cycle. The agreement between the solutions obtained when using 20 steps

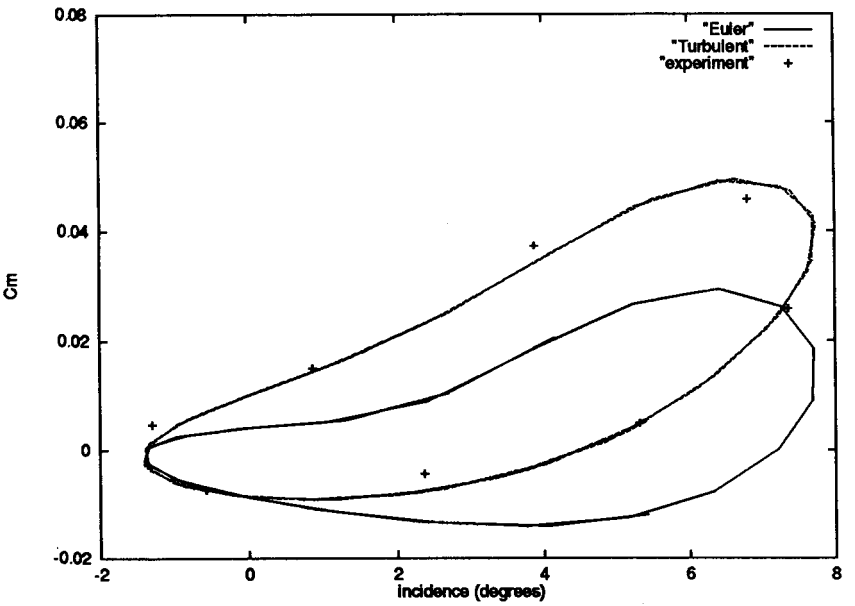

Figure 6. Predicted inviscid and turbulent histories for integrated moment for case CT2.

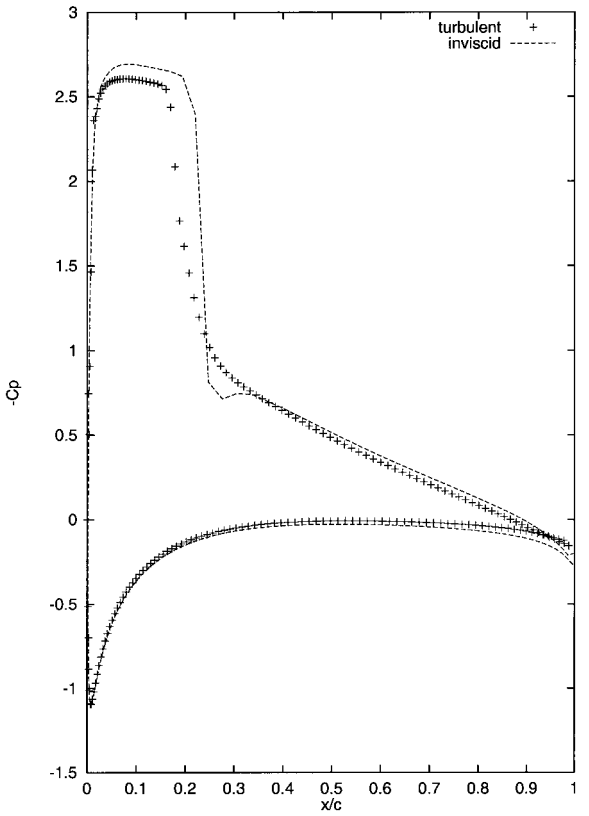

Figure 7. Predicted inviscid and turbulent pressure distributions for case CT2.

per cycle for sequencing in real and pseudo-time is close up to the time when the solution which is sequenced in real time fails. This happens at the edge of the boundary layer after the shock wave where the large changes in flow values between real time steps due to the shock motion cause problems when frozen flow values are used. The difference between the coupled and sequenced solutions is largest in the boundary layer after the shock wave. The solution obtained when using 40 steps per cycle for real and pseudo-time sequenced solutions compare well, suggesting that the main effect of using a sequenced solution in real time for this case is on robustness and not accuracy, i.e. when the sequencing has an influence it causes the calculation to fail.

For the ramping case, no solution is obtained beyond stall when sequencing in real time for time steps resulting in a motion of greater than 0.170°. The solution that was obtained when sequencing in real time for a smaller time step (0.085° per step) is well converged with respect to the time step. Convergence is achieved at a larger time step when sequencing in pseudo-time (0.170° per step), suggesting that there is a reduction in accuracy from using the real time sequencing for this case.

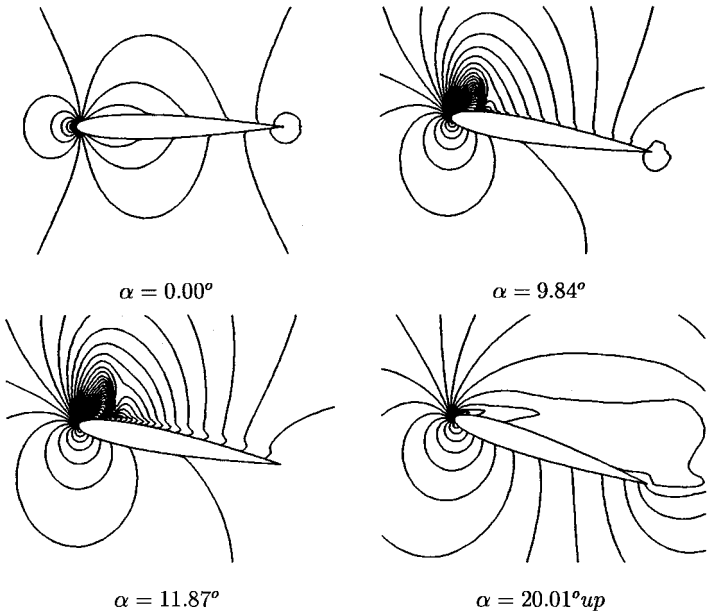

Figure 8. Pressure contours for case CT8.

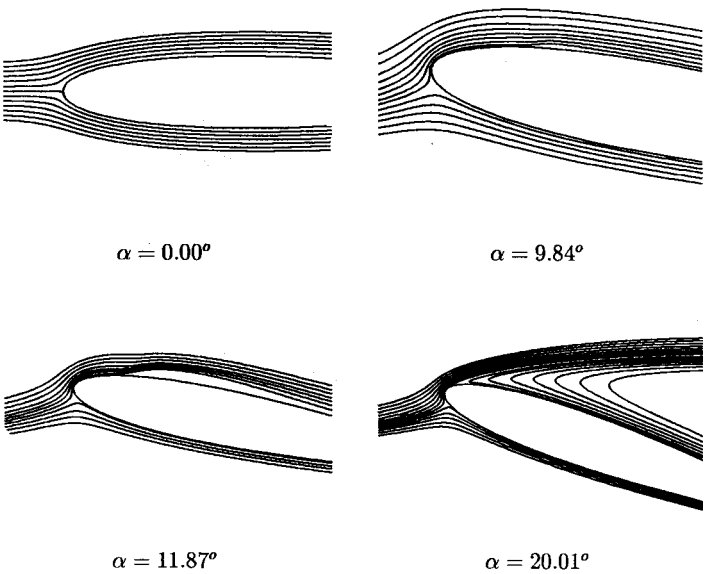

Figure 9. Streamlines for case CT8.

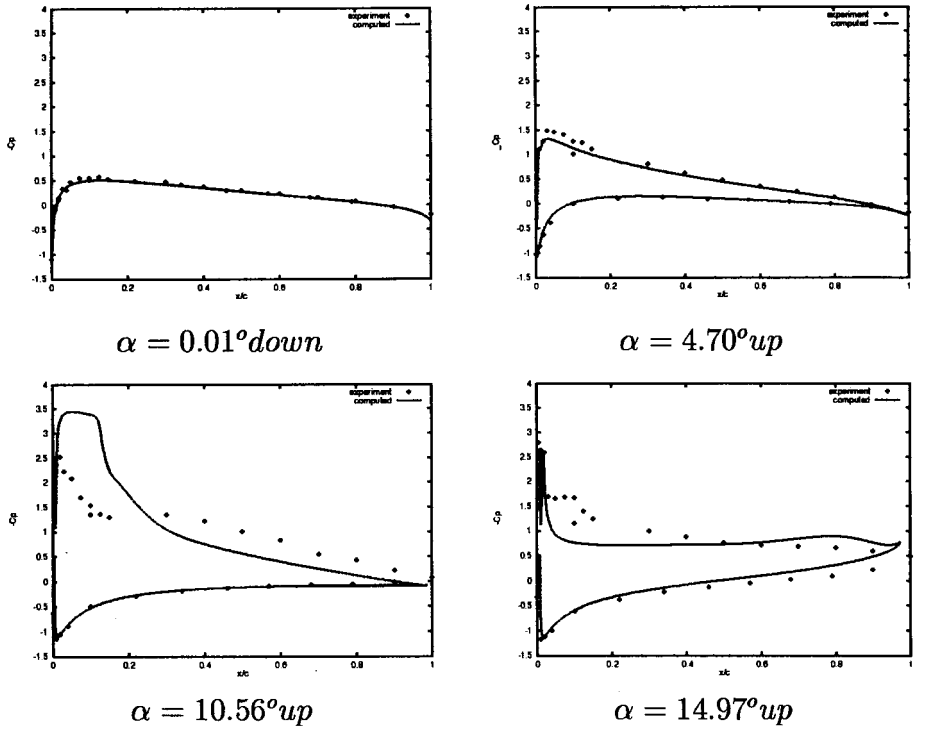

Figure 10. Instantaneous pressure distributions for case CT8.

There are, therefore, two malign effects encountered for these test cases when sequencing the solution in real time. First, when a shock motion is the most important feature in the flow the sequencing leads the solution to fail for large time steps. This can be explained by the large changes in flow values due to shock motions causing large errors if variables are frozen. For the ramping case a reduction in accuracy is noted as well, which is due to the significant changes in the flow in the separated region leading to errors if values are frozen. These errors are not large enough to cause the solution to fail, as is the case when shock motions are present.

It is interesting to observe the influence of the coupling on the pseudo-steady state convergence. Using 40 steps per cycle for the pitching case the average number of pseudo-steps per real time step required for the mean flow solution sequenced in real and pseudo-time is almost identical. This indicates that the solution coupling when using sequencing in pseudo-time does not make the mean flow pseudo-steady state problem significantly harder. This is due to the small influence that a small change in a diffusion coefficient (the eddy viscosity) is likely to have on the mean flow solution. However, the turbulent solution is observed to be 20 pr cent slower when the solutions are sequenced in pseudo-time. This reflects the much larger influence on the solution that changing values of ρ, u and v during the iteration in the conserved variables, convective and diffusive fluxes and the source term is likely to have on the

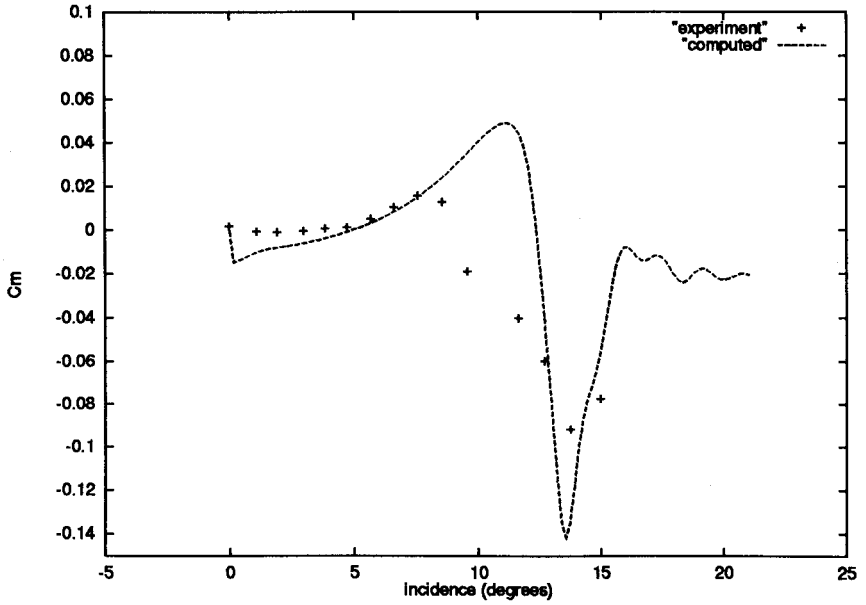

Figure 11. Comparison of integrated moment with experiment for case CT8.

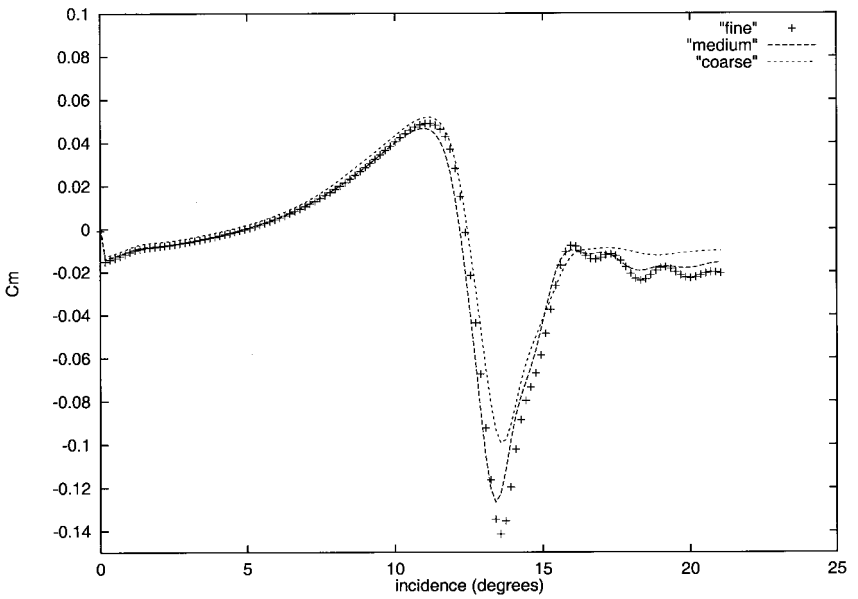

Figure 12. Grid convergence for integrated moment for case CT8.

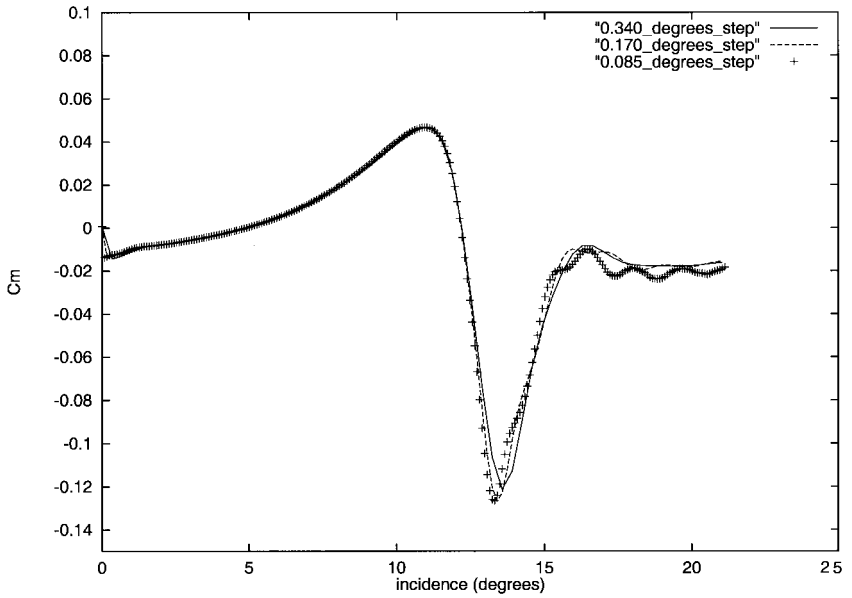

Figure 13. Convergence with number of real time steps per cycle for integrated moment for case CT8.

convergence of k and ω. It should be noted, however, that since we can obtain an accurate solution using 20 steps per cycle using the solution which is sequenced in pseudo-time as compared with 40 steps per cycle for the real time sequenced method, the pseudo-time sequenced method still shows a clear advantage in terms of efficiency. Similar conclusions apply for the ramping case.

Table I. Effect of the size of the time step on the flow solver efficiency.

Case	Number of time steps	Average number of pseudo-time steps per real time step	CPU time (in work units)
CT2	80/cycle	31	5666/cycle
Medium grid	40/cycle	36	3265/cycle
	20/cycle	44	1956/cycle
	10/cycle	54	1209/cycle
CT8	0.042°/step	18	12 528
Medium grid	0.085°/step	23	8074
	0.170°/step	29	5196
	0.340°/step	36	3343

7. CONCLUSIONS

Results for the turbulent flow over the NACA0012 aerofoil in pitch and ramp have been presented. These test cases have been used to assess various aspects of the numerical method used for the simulation.

The main conclusions for the current method and test cases are:

- The pseudo-time iterations can be stopped when the pseudo-time update has been reduced to less than 1 per cent of the corresponding real time update.

Table II. Effect of grid refinement on the flow solver efficiency.

Case	Grid	Average number of pseudo-time steps per real time step	CPU time (in work units)
CT2	Coarse	27	1154/cycle
20 steps/cycle	Medium	44	1956/cycle
	Fine	63	2840/cycle
CT8	Coarse	23	3557
0.170°/step	Medium	29	5196
	Fine	42	5341

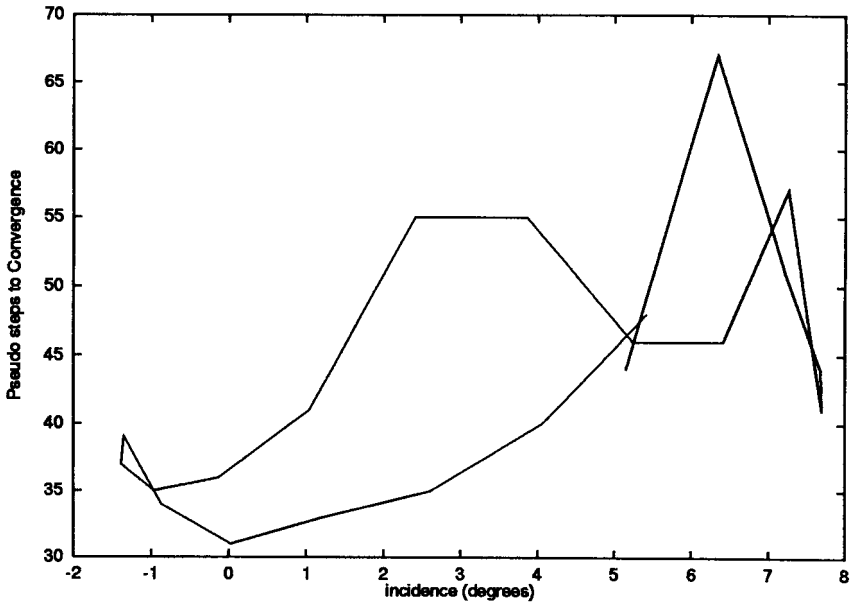

Figure 14. Pseudo-steps required at points around the pitching cycle for CT2 using CFL = 50 and approximately 20 real time steps per cycle.

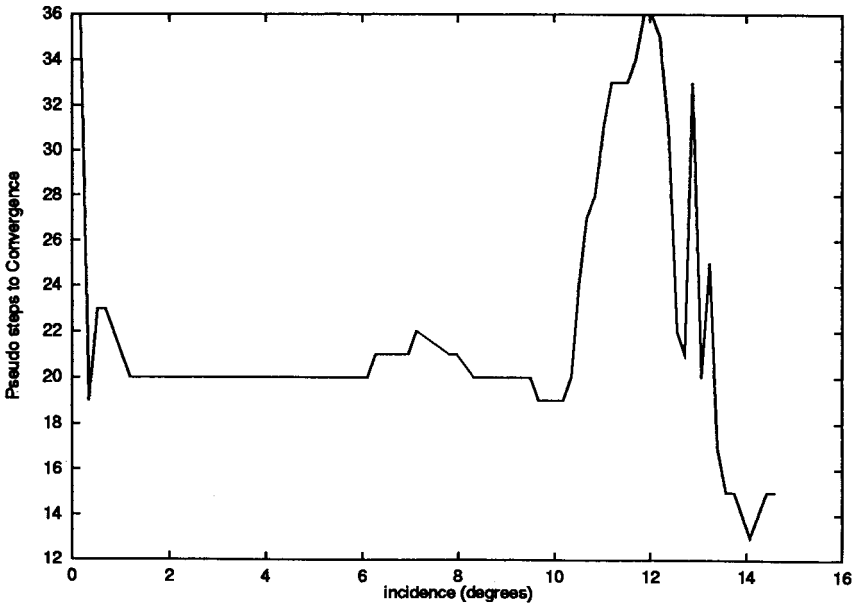

Figure 15. Pseudo-steps required at points during the ramping cycle for CT8 using CFL = 100 and 0.170° per step.

- The safest initial iterate for the pseudo-time solution is the converged solution from the previous time step, using an extrapolated solution can lead to robustness problems when using large time steps.
- Solution sequencing in pseudo-time is preferable to sequencing in real time from an accuracy and robustness point of view.
- The cost of solving the mean flow problem is very similar, whether the solution is sequenced in real or pseudo-time.
- Shock motions increase the expense of the pseudo-time solution, flow separation does not for the current cases.
- Using a moment centre at the location given in the experimental description of the pitching test case gives good agreement with measured values, in contrast to Euler results.

The promise of doing time-accurate turbulent flow simulations within the pseudo-time framework has been demonstrated. The generality of these conclusions for more complex test cases is being tested.

ACKNOWLEDGMENTS

The authors acknowledge the support of British Aerospace and the Defence and Evaluation Research Agency who jointly supported the investigation of solution methods for unsteady flows, and the UK LINK programme on Advanced Rotorcraft Technologies supporting the helicopter applications of this research. They would also like to thank the other members of the CFD group at Glasgow for their invaluable assistance during this work, and particularly Daniel Feszty for preparing some of the figures.

APPENDIX A. NOMENCLATURE

c	aerofoil chord
C_m	pitching moment coefficient
e	total energy
$\mathbf{f}^i$, $\mathbf{g}^i$	convective fluxes for mean flow
$\mathbf{f}^v$, $\mathbf{g}^v$	diffusive fluxes for mean flow
$\mathbf{f}_T^i$, $\mathbf{g}_T^i$	turbulent convective fluxes
$\mathbf{f}_T^v$, $\mathbf{g}_T^v$	turbulent diffusive fluxes
k	turbulent kinetic energy
k_r	$\mathrm{d}\alpha/\mathrm{d}t$ for ramping case
$\mathbf{Q}_{i,j}$	turbulent flow flux residual
$\mathbf{Q}_{i,j}^*$	turbulent flow unsteady residual
$\mathbf{R}_{i,j}$	mean flow flux residual
$\mathbf{R}_{i,j}^*$	mean flow unsteady residual
$\mathbf{q}$	turbulent conservative variables
$\tilde{\mathbf{q}}_{i,j}$	vector of conserved turbulent variables in cells which contribute to $\mathbf{Q}_{i,j}$
$\mathbf{S}$	turbulent source term
t	time
u, v	Cartesian velocity components
$\mathbf{w}$	mean flow conservative variables
$\tilde{\mathbf{w}}_{i,j}$	vector of conserved mean flow variables in cells which contribute to $\mathbf{R}_{i,j}$
x, y	Cartesian co-ordinates

Greek letters

α	angle of attack
α_m	mean angle
α_0	amplitude of oscillation
μ_t	eddy viscosity
ρ	density
ω_p	angular frequency
ω	turbulent dissipation rate of k
Δt	real time step
$\Delta\tau$	pseudo-time step

Subscripts

i, j	computational cell
∞	freestream conditions

Superscripts

m	time level of the approximation in pseudo-time
n	time level of the approximation in real time

REFERENCES

1. Jameson A. *Time dependent calculations using multigrid, with applications to unsteady flows past airfoils and wings*. Technical Report AIAA 91-1596, 1991.
2. Gaitonde AL. A dual-time method for the solution of the unsteady Euler equations. *Aeronautical Journal* 1994; **10**: 283–291.
3. Venkatakrishnan V, Mavriplis DJ. *Implicit method for the computation of unsteady flows on unstructured grids*. 12th AIAA Computational Fluid Dynamics Conference, San Diego, CA. AIAA 1995; 675–686.
4. Dubuc L, Cantariti F, Woodgate M, Gribben B, Badcock KJ, Richards BE. Solution of the Euler unsteady equations using deforming grids. *AIAA Journal* 1998; **36**: 1417–1424.
5. Cantariti F, Dubuc L, Gribben B, Woodgate M, Badcock KJ, Richards BE, McMillan WS. Integration of an implicit multiblock code into a workstation environment. In *Parallel Computational Fluid Dynamics*, *Recent Developments and Advances Using Parallel Computers*, Schiano P *et al*. (eds). North-Holland: Amsterdam, 1998; 169–176.
6. Gribben B. *Application of the multiblock method in computational aerodynamics*. Ph.D. Thesis, Department of Aerospace Engineering, University of Glasgow, 1999.
7. Ekaterinaris JA. Numerical investigation of dynamic stall of an oscillating wing. *AIAA Journal* 1995; **33**: 1803–1808.
8. Simpson LB, Whitfield DL. Flux-difference split algorithm for unsteady thin-layer Navier–Stokes solutions. *AIAA Journal* 1992; **30**: 914–922.
9. Ko S, McCroskey WJ. Computation of unsteady separating flows over an oscillating airfoil. *AIAA Journal* 1997; **35**: 1235–1238.
10. Hamed A, Shih SH, Yeuan JJ. Unsteady supersonic cavity flow simulations using coupled $k-\epsilon$ and Navier–Stokes equations. *AIAA Journal* 1994; **32**: 2015–2021.
11. Damodaran M, Jiang YT, Lee KH. High resolution finite volume computation of turbulent transonic flow past airfoils. *AIAA Journal* 1997; **35**: 1134–1142.
12. Cantariti F, Dubuc L, Gribben B, Woodgate M, Badcock KJ, Richards BE. *Approximate Jacobians for the solution of the Euler and Navier–Stokes equations*. Aerospace Engineering Report, 5, Glasgow University, 1997.
13. Wilcox DC. *Turbulence Modelling for CFD*. DCW Industries: La Canada, CA, 1993.
14. Olsen JJ. *Compendium of unsteady aerodynamic measurements*. Technical Report 702, AGARD, 1982.
15. Gaitonde AL, Fiddes SP. A comparison of a cell-centre method and a cell-vertex method for the solution of the two-dimensional unsteady Euler equations on a moving grid. *Proceedings of the Institution of Mechanical Engineers Part G: Journal of Aerospace Engineering* 1995; **209**: 203–113.
16. Allen CB. Central-difference and upwind-biased schemes for steady and unsteady Euler aerofoil calculations. *Aeronautical Journal* 1995; **99**: 52–62.
17. Badcock KJ, Gaitonde AL. An unfactored implicit moving mesh method for the two-dimensional unsteady Navier–Stokes equations. *International Journal for Numerical Methods in Fluids* 1996; **23**: 607–631.

